Intrinsic resolutions of DEPFET detector prototypes measured at beam tests

Laci Andricek[a], Javier Caride[b], Zdeněk Doležal[c], Zbyněk Drásal[c], Simone Esch[d], Ariane Frey[e], Julia Furletova[d], Sergey Furletov[d], Christian Geisler[e], Stefan Heindl[f], Carmen Iglesias[b], Jochen Knopf[g], Manuel Koch[d], Peter Kodyš[c1], Christian Koffmane[a,i], Christian Kreidl[g], Hans Krüger[d], Peter Kvasnička[c], Carlos Lacasta[h], Lukáš Malina[c], Carlos Mariñas[h], Jelena Ninkovic[a], Lars Reuen[d], Rainer Richter[a], Stefan Rummel[a], Ján Scheirich[c], Johannes Schneider[d], Benjamin Schwenker[e], Pablo Vazquez[b], Marcel Vos[h], Thomas Weiler[f], Norbert Wermes[d],

[a] MPI Munich, Germany
[b] Santiago de Compostela University, Spain
[c] Institute of Particle and Nuclear Physics, Faculty of Mathematics and Physics, Charles University in Prague, Czech Republic
[d] Bonn University, Germany
[e] Göttingen University, Germany
[f] KIT Karlsruhe, Germany
[g] University of Heidelberg, Institute for Computer Engineering, Mannheim, Germany
[h] IFIC, centre mixte Universitad Valencia/CSIC, Spain
[i] TU Berlin, Faculty of Electrical Engineering & Computer Science, Sensor & Actuator Systems, Germany

Abstract - Intrinsic resolution is the root-mean-square error of position measurement in the detector. Using the knowledge of multiple scattering statistics, the contributions of multiple scattering and position measurement errors in tracking residuals can be disentangled, and intrinsic resolutions can be estimated.

This paper uses the data of the 2009 DEPFET beam test at CERN SPS. The beam test used beams of pions and electrons with energies between 40 and 120 GeV, and the sensors tested were 450 μmthick prototypes with pixel pitch between 20 and 32 μm. We introduce the intrinsic resolution calculations and demonstrate some properties of resolution estimates and factors that influence them. For the DEPFET detectors in the beam test, we get intrinsic resolutions of $\approx$ 1 μm, with typical accuracy of 0.1 μm. We use the bias scan, angle scan,a and energy scan to show that resolutions are a useful tool in the study of detector properties. We also show that detailed resolution maps can be constructed when precise telescopes are available.

[1]The corresponding author Peter Kodyš is with the Faculty of Mathematics and Physics, Institute of Particle and Nuclear Physics, Charles University, V Holesovickach 2, 18000 Prague, Czech Republic (e-mail: peter.kodys@mff.cuni.cz), tel: +420 221 912 453, +420 221 912 761

1 Introduction

Experiments in future colliders like the ILC or the super B factories require excellent vertexing performance. The DEPFET collaboration pursues the development of vertex detectors based on the concept of the depleted field effect transistor.

The concept (see Fig. 1) originated in the 1980s and has been published widely [1]-[4]. Briefly, each DEPFET pixel has an integrated p-FET transistor. Sideward depletion creates a potential minimum for electrons in the internal gate under the channel. Electrons collected in the internal gate modulate the transistor current. They can be removed from the internal gate via the clear contact.

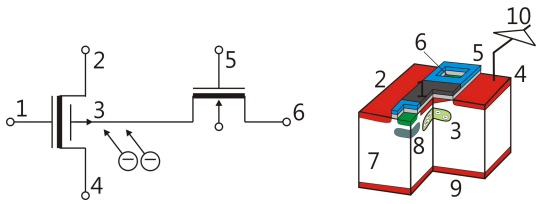

Figure 1: The principle of DEPFET. 1 - external FET gate, 2 - p^+ source, 3 - deep n-doped internal gate, 4 - p^+ drain with connection to external amplifier, 5 - clear gate, 6 - n^+ clear, 7 - depleted n-Si bulk, 8 - deep p-well, 9 - p^+ backside contact, 10 - amplifier

Currently, two major application areas for the DEPFET-based detectors are imaging systems of space based X-ray astronomy missions (XEUS, SIMBOLX, BepiColombo) and vertex detectors in high-energy physics colliders (the Belle II at KEK and the ILC). The challenging requirements on state-of-the-art vertex detectors combine excellent vertex reconstruction, achievable only by a highly granular pixel detector, with fast readout and minimum material budget to reduce the impact of multiple Coulomb scattering on the measurement. This severely constrains sensor thickness, power consumption and design of detector services.

In summer 2009, eight latest DEPFET prototype modules were tested in the pion and electron beams at CERN's Super Proton Synchrotron (SPS). The modules were fully depleted DEPFET active pixel sensors designed for the ILC vertex detector, with several pixel pitch options [5].

The present paper contains beam test results with special focus on intrinsic resolution of DEPFET detectors. We define the intrinsic resolution of a detector as the root-mean-square error of position measurement in the detector. The reason for a separate paper on intrinsic resolutions is their importance not only *per se* as a measure of accuracy of the positional information provided by the detector, but also as a versatile tool for studies of various detector properies (such as detector depletion voltage and charge sharing) and analysis procedures (such as hit reconstrution or alignment).

Systematic studies of DEPFET spatial resolutions started in 2006 by Jaap Velthuis et al. [6], and continued in the following years [7].

Estimation of intrinsic resolutions is a relatively straightforward procedure, though somewhat numerically subtle: the task is to decompose the tracking residuals to contributions of multiple scattering and measurement errors, based on known statistics of both.

We give a fairly extensinve description of beam test data analysis with a view to showing how individual steps of the analysis, such as hit reconstruction, alignment and tracking, mechanical instabilities, and irregularities in detector response, influence intrinsic detector resolutions. A few results of a MC simulation study illustrate the consistency of resolution estimates.

We illustrate the usefulness of detector resolutions by showing the results of beam energy scan, bias scan and angle scan in terms of detector resolutions. Some results on the variation of detector resolutions within the area of a detector pixel illustrate another useful application.

2 DEPFET beam test

The 2009 DEPFET beam test setup was built of 6 detectors as close to one another as allowed by the position stages to minimize the effects of multiple scattering. Particles were triggered by two scintillators in front of and behind the setup.

Five matrices of the same type were used as telesopes. Their parameters were kept constant during beam test experiments. The Detectors Under Tests (DUT) were three structures designed specially for the ILC conditions, with small pixels and high resolution. The thickness of all matrices was 450 μm. Eight matrices with 64 $\times$ 256 pixels, pixel pitch 20 $\times$ 20, 24 $\times$ 24 or 32 $\times$ 24 μm were used.

The geometry of the 2009 beam test is shown in Fig. 2. The DUT was placed in position 2.

Fig. 3 shows orientation of the (local) detector coordinate system relative to the layout of chips on a DEPFET hybrid.

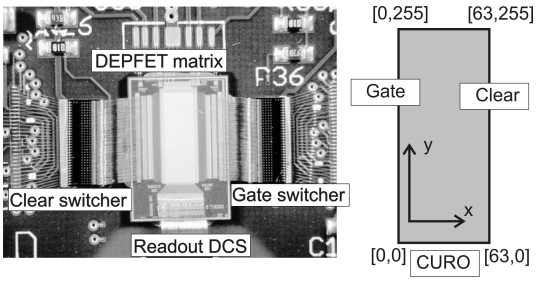

Figure 3: Layout of chips on a hybrid and the detector coordinate system

The six detectors of the setup were synchronized with a EUDET Trigger Logic Unit and operated from a Linux workstation.

We found tracks passing through all six detectors in ≈25% events, the inefficiency being mainly due to triggering by a 2.4 $\times$ 6.5 mm^2 scintillator at the front of the setup. Typical acquisition rate with 120 GeV pion beam was higher than 1000 events per minute.

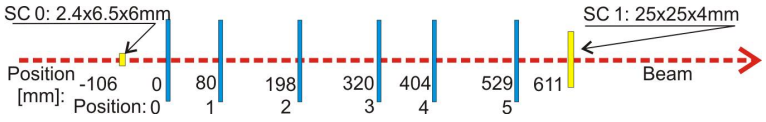

Figure 2: Arrangement of sensors in the 2009 beam test

The basic set of beam test studies comprised bias scan, 100 to 200 V; angle scan, ±4 deg tilt of the DUT around horizontal axis[2]; energy scan, 40 to 120 GeV, separate runs with electron beams with energies 40, 60, 80, and 100 GeV, and pion beams with energies 80, 100, and (default) 120 GeV.

3 Specific properties of DEPFET detectors

DEPFET detectors have some special features that have to be explained in order to understand the beam test analysis and its results.

3.1 Noise and intrinsic resolution

In DEPFET detectors, noise is dominated by the front-end electronics and was about 120 nA for all detectors where typical amplification in pixel is about 0.5 nA/e$^-$. Response to 120 GeV pions (110 keV deposited energy) was over 14.6 μA for the large pixel pitch (signal to noise ratio about 120), and 25.3 μA for the small pixel pitch (signal to noise ratio 200) [8]. In combination with fine pitch, the high S/N ratios result in intrinsic resolutions between 1 and 2 μm (see the Results section below). With these parameters, multiple scattering effects are very important at the nominal beam energy of the beam test, 120 GeV, and become dominant at the lower beam energies (down to 40 GeV) used in the energy scan.

3.2 Pixel structure

The elementary cell of a DEPFET matrix comprises 1 × 2 pixels as shown in Fig. 6: indeed, for the fine coordinate (y, the dimension with 256 pixels) a pattern with 2-pixel period can be identified in the sensor design, see Fig. 4. The "large ILC" pixel design (Fig. 4, right) was used in telescopes, and the "smallest ILC" and "small ILC" pixel designs (Fig. 4 left and center) were used for the DUTs (module 2). Data analysis has to respect this specific feature, for example, in the calculation of η corrections.

3.3 Edge effect and other positional response distortions

The edge effect is a small shift of charge generated by particles in the detector bulk towards the perimeter of the detector's active area. It has been observed in all

[2]The angle scan was actually performed at the 2008 DEPFET beam test that took place at the same site and with similar setup.

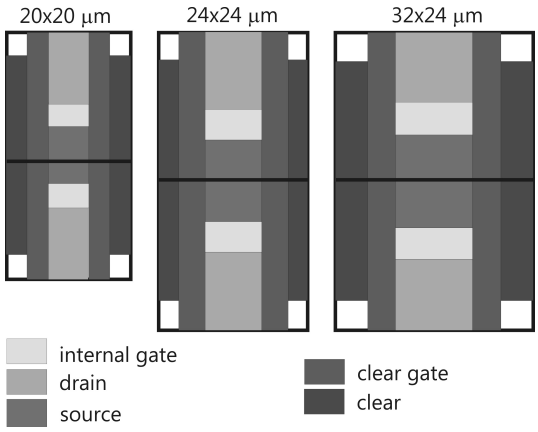

Figure 4: The design of a 1 × 2 pixels area for the smallest (left), small (center) and large (right) ILC pixel design.

DEPFET beam tests as a systematic bias in the positional information reported by detectors. Later it was confirmed by laser tests. The distortion affects a zone of up to 250 μm around the perimeter of a detector's active area. The effect arises from a potential difference between the interior of the detector's active area and the outer ring, the latter potential being higher by about +10V. An appropriate setting of the outer ring voltage can suppress the effect. Other types of response distortions have been observed in previous beam tests. They include V-effects (shift between the two halves of a sensor) and periodic distortions. They are less pronounced and are corrected in the same way as edge effects. By careful configuration of detector settings, they were strongly suppressed in the 2009 beam test.

4 Data analysis

Beam test data were analyzed by three independent groups (universities of Bonn, Göttingen and Prague) using different approaches and software tools. The results were cross-checked up to the level of tracking residuals and all discrepancies between the results of the three groups have been thoroughly investigated and are currently well understood. The presentation of the analysis chain in this section refers to the analysis of the Prague group.

4.1 Data analysis chain

The data analysis chain comprised the following steps:

Raw data inspection and frame display: check consistency and arrangement of data; identify exposed regions on detectors; mask channels with wrong response

Black correction: estimate pedestals and common mode noise (CMN) as medians of signals; subtract pedestals and

CMN from frame data; estimate RMS channel noises as median absolute deviations of channel signals

White correction: estimate pixel gains using semi-parametric maximum-likelihood equalization of seed distributions; pixel gains are applied in hit reconstruction when a reliable value reliably different from 1 is available

Hit reconstruction: identify signal clusters; estimate hit positions using center of gravity and eta correction (see below in the list) based on groups of 2 × 2 (large pixel size) or 3 × 3 (small pixel size) highest signals of a cluster

Track formation: combine hits on various detectors into particle tracks using the Scott and Longuet-Higgins [9] similarity matrix deconvolution. Only tracks with exactly one hit in every sensor (and hits belonging to such tracks) are used in the following analysis

η corrections are calculated using only hits that belong to tracks; two one-dimensional η corrections [10] are calculated for the x and y projections of 2×2 pixels' area for each sensor

Track fitting and sensor alignment: parameterize particle tracks; estimate intersections of tracks with detectors; correct for detector misalignment. A cut of 250 μm around the perimeter of each detector was used to eliminate edge effects

Correction for mechanical movements: regularly update alignment to account for slow mechanical changes in detector positions (typical time scale tens of minutes). See 5.2 for more details.

Correction of response distortions: use patterns in tracking residuals to correct for systematic bias of the detector's positional response. See 5.3 for more details.

Calculation of detector resolutions: estimate detector resolutions, tracking errors, telescope resolution at DUT plane, etc. See 5.1 for more details.

4.2 Analysis software

Two analysis groups (Bonn and Göttingen) used the ILCSoft/EUTelescope [11] analysis package with special extensions for DEPFET sensors [12]. One group (Prague) used their own ROOT-based [13] analysis package allowing also intrinsic resolution calculations.

5 Notes on selected analysis methods

This section gives some more detail on selected steps of the analysis. The level of detail for individual steps was chosen in correspondence with the focus of the paper.

5.1 Calculation of detector resolutions

By *detector resolution* we mean the RMS error of position measurement in the detector. We calculate detector resolutions from the covariance matrix of track fit residuals. Each fit residual is a linear combination of detector measurement errors and multiple scattering deflections. Therefore, residual covariance is a linear combination of measurement error covariance and multiple scattering covariance:

$$cov(\hat{u}^c) \equiv \left\langle (u^c - \hat{u}^c)(u^c - \hat{u}^c)^T \right\rangle = H(G\Sigma^2 G^T + \Delta^2)H \quad (1)$$

where:

- u^c are local hit coordinates and $\hat{u}^c$ are local coordinates of track intersection with sensor plane
- H is a projector to the residual space. If the track is fitted with a line, $u = F\beta$, with F the factor matrix and β the vector of line intercepts and slopes, then $H = I - F(F^T F)^{-1} F^T$
- G describes the geometry of multiple scattering. In the simplest case, $G_{ij} = (z_j - z_i)_+$ with z_i being the z coordinate of the i-th detector
- Σ and Δ are diagonal matrices of multiple scattering deflections and squared detector resolutions

RMS multiple scattering deflections in Σ can be calculated using the Moliére formula, so we can express detector resolutions in Δ in terms of (experimental) residual correlations and (theoretical) RMS multiple scattering deflections.

Formally, resolutions can be calculated by solving 1 for Δ. The procedure is complicated by the fact that H doesn't have full rank: its rank is 2 × (number of points on the track) - 4. We can use some matrix algebra to express the resolutions in terms of pseudoinverses of HH, which is equivalent to a least-squares fit to the covariance matrix. This gives us the "diagonal" estimator; when the type of resolution estimator is not specified in this report, than this estimator is meant.

Another, more straightforward method is to find the resolutions by a maximum likelihood fit to the data using a non-linear fitter. Such estimate uses the full covariance matrix, but to-date it doesn't seem to be decisively better than the "diagonal" estimator. It is significantly more stable than the "diagonal" estimator in the large multiple scattering regime, but in that regime both estimators behave very poorly.

A strong test of the quality of intrinsic resolution estimates is by varying detector setup. If we omit data from a selected module from the analysis (keeping the module in the setup, however, as passive material and a source of multiple scattering), we expect the same resolutions on the remaining detectors as with the "full" setup - except, possibly, with a larger statistical error. We however observe some systematic, geometry-dependent deviations in these calculations. They are most likely related to poor numerical properties of the problem - we are effectively inverting an ill-conditioned matrix. For example, in the 2009 beam test, the typical systematic error was 0.1 μm in both coordinates.

The key test of resolution estimates is beam energy scan. It allows to use the traditional method of resolution calculation by extrapolation to zero multiple scattering, the

so-called "infinite energy extrapolation". Since this is a "cleaner" method in that it does not rely on a specific model of multiple scattering, it is a good reference for the quality assessment of resolution estimators. Unfortunately, we have repeatedly found that a practical realization of the energy scan with a sufficiently broad range of beam energies at CERN's SPS is by itself a difficult task, as will be discussed later in the corresponding Results section.

5.2 Mechanical stability

Mechanical instabilities degrade the observed intrinsic resolution of detectors. There are at least two sources of mechanical instabilities: (i) slight movements of setup elements in response to changes in ambient temperature or humidity; (ii) mechanical transients arising from slowly relaxing stresses in positioning stages, cabling etc. The obvious way of improvement of the situation is to use stiffer mechanics. The other way is to use sliding alignment. The achievable improvement is given by sample size behaviour of alignment precision and by the rate of mechanical misalignment. With the mechanical drift rate unchanged, the efficiency of re-alignment depends on the track acquisition rate: when track rate is small, the alignment has to be averaged over longer time intervals. A simplified re-alignment procedure was used in the beam test analysis: only shifts of detectors perpendicular to the beam (x and y) were updated. They were calculated as median residuals in residual plots (that is, plots of residuals vs. coordinate).

5.3 Correction of edge effect and other response distortions

Similarly to instabilities in time due to mechanical drifts, irregularities in the positional response of DEPFET sensors were observed as patterns of systematic bias in residual plots. Such irregularities shift space points by tenths of microns to microns. The correction simply subtracts median residuals (accross a run) for each position from the residuals of individual track fits.

5.4 Sub-pixel analysis

The high resolution of the telescope system and available analysis methods allowed us to map variations of detector properties within a pixel. To calculate the response from a point within a pixel, a weighted average of 4,000 closest tracks was calculated. The response was calculated on a grid of 9 $\times$ 18 points inside the area of the elementary cell (1$\times$2 pixels) of the sensor matrix. We present here resolution maps.

5.5 Monte Carlo simulations

Verification of analysis and validation of resolution estimates on simulated data serves as an important crosscheck of the analysis methods and results. Simulations are even more "intrinsic" to the analysis - it is often the only or the most convenient way of estimating errors and sensitivity of analysis. The "full" simulations of particle tracks in the beam test setup were carried out using the ILC software framework [14]: the beam test setup was included in the Mokka database and particle tracks were simulated by the GEANT4 engine. No digitization was used; instead, detector intrinsic resolutions were imitated by Gaussian smearing. A simple Marlin module was used to convert the LCIO data to ROOT trees. The simulated data underwent the same analysis as real data, starting from the track formation stage (cf. 4.1).

6 Results and discussion I: Resolutions

Tracking residuals are key pre-requisites for the calculation of alignment (including corrections of mechanical movements), response distortion corrections, and resolutions. In this paper, "residuals" always mean "unbiased" residuals, that is, residuals from track fits using hits in all other modules except the module in question.

Table 1 shows a comparison between residuals for all detectors obtained in the analyses of the Prague and Goettingen groups. The analyses were carried out independently, using different algorithms (for example, for eta correction and for alignment) and different software (see section 4.2). The agreement in residuals is apparent. We note that agreement in residuals means agreement in resolutions, so the results presented in the following sections were confirmed by two independent analyses. For clarity, we quote in the following the Prague group values.

residuals [μm]	0	1	2	3	4	5
Göttingen x	2.39	1.52	1.46	1.81	1.97	2.86
Prague x	2.49	1.60	1.54	1.98	2.06	3.24
Göttingen y	2.24	1.27	1.42	1.55	1.60	2.89
Prague y	2.28	1.38	1.42	1.61	1.61	2.86

Table 1: Comparison of residuals for individual detectors obtained in two independent analyses by the Prague and Göttingen groups for all 6 modules. The analyses used 1600 events taken with DUT with pixel size 20 $\times$ 20 μm^2 in position 2.

6.1 Values

The values of residuals and intrinsic resolutions for two modules (DUT with pixel size 20 $\times$ 20 μm^2 in position 2 and a telescope with pixel size 32 $\times$ 24 μm^2 in position 3) are shown in Table 2. The table also shows estimates of net tracking error (error of the telescope system in the limit of zero multiple scattering) and RMS contribution of multiple scattering to residual for 120 GeV pions. Telescopes at other positions of the setup were of the same type and have, within experimental error, the same intrinsic resolutions.

[μm]	Module 2 (DUT) 20×20 μm^2		Module 3 (telescope) 32×24 μm^2	
	x	y	x	y
Residual	1.54	1.42	1.98	1.61
Resolution	1.10	1.00	1.60	1.20
Net Tracking Error	0.73	0.62	0.86	0.73
Multiple Scattering	0.76		0.79	

Table 2: Typical residuals and resolutions in x and y for 120 GeV pions. Systematic error is 0.1 μm. Residuals and resolutions are representative for several combinantions of conditions and algorithms.

6.2 Monte Carlo verification

Results of MC studies are shown in Fig. 5. Fig. 5 shows the resolutions extracted from the real and simulated data by the analysis. Apparently, in the low multiple scattering regime with the 120 GeV beam, the analysis reproduces the true values with satisfactory precision.

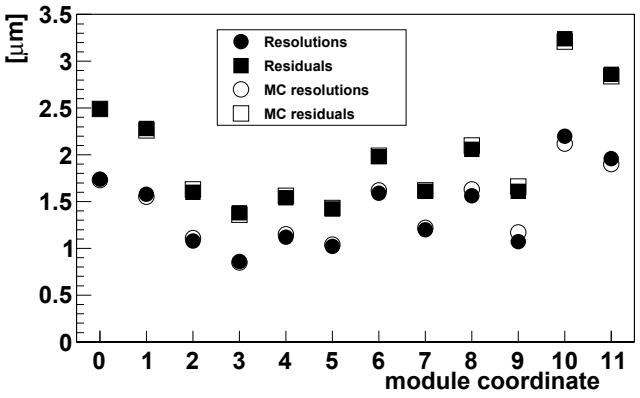

Figure 5: Comparison of residuals (squares) and resolutions (circles) from the analysis of beam test data (solid) and simulated data (hollow) with representative resolutions set for all detectors (120 GeV pion beam)

6.3 Factors influencing the intrinsic resolutions

Several factors can degrade the observed intrinsic resolutions. Fortunately, most distortions lead to worse (numerically larger) resolutions than the true ones [3], so usually a decrease in observed resolutions means an improvement in analysis.

Gain correction An uncertainty in pixel gains directly affects position resolution: when calculating COG from 2 pixels, 1% error in gain leads up to 0.5% error in position, equivalent to 0.5% of pitch - that is, tenths of microns, which is measurable. To measure such a small difference in gains, however, we have to equalize distributions of 10^4 signals. For large pixel arrays, this means really huge statistics that may be pretty tricky to achieve.

In beam test 2009, we were able to calculate pixel gains with about 4% precision, which was about the level of spread of actual pixel gains, so application of gains gave no visible improvement in resolutions.

Hit reconstruction Centre-of-gravity (COG) position estimates for signal clusters were calculated from 2 × 2 pixels with largest summary signal in a cluster. This gives best results for detectors with average cluster size less than 2 in every axis, or with full cluster size less than 4. For approximatelly perpendicular tracks of particles and modules with thickness of 450 μm, this condition is usually fulfilled for pixel sizes over 24 × 24 μm^2. One DUT module has a smaller pixel size (20 × 20 μm^2) and its average cluster size exceeded 2 × 2. For this module, the best resolution was obtained for COG calculated from 3 × 3 pixels (or from the full COG calculation).

For position calculation, only pixels with signals over 2.6 × average noise were accepted. For every direction, position and its error were calculated independently as signal- and noise-weighted means and standard deviations. As already mentioned, η corrections are applied as two independent one-dimensional η corrections in both coordinates. They are calculated in the traditional manner [10], with the exception that, in each direction, hit occupancy is equalized over two pixels rather than one. This is due to the specific structure of the DEPFET sensor matrix, see 3.2, and it is a smarter variant of using two separate η corrections for odd and even pixels. Examples of typical η correction functions are shown in Fig. 6. The asymmetry mentioned in 3.2 manifests clearly in these plots: in the y direction (right plot) there is, for every module, a visible shift upwards with respect to the symmetrical value expected in case of equal pixels.

The efficiency of "double-pixel" η correction compared to a "single-pixel" η is clearly visible in intrinsic resolutions.

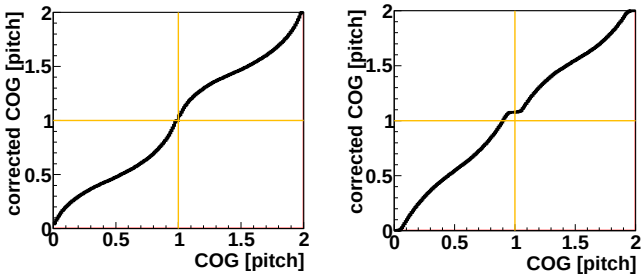

Figure 6: Example of η correction functions in x(left) and y (right) directions

Mechanical stability

With longer acquisition times, mechanical instabilities of the detector setup become an issue. The solution is to re-calculate alignment regularly during the run. The frequency of re-alignment is given by the number of tracks needed to calculate a reasonably precise (correction of) alignment. This is about 1000 tracks for the DEPFET beam test setup. Thus, the limit of improvement are misalignment drifts ocurring within the time needed to acquire 1000 particle tracks. This is about 4.5 minutes for 120 GeV pions, but 61 minutes for 40 GeV electrons. Therefore, the results for electrons are much more likely to be affected by slow variations in the setup.

[3] An important counter-example is biased sampling, such as tight cuts on fit χ^2.

An 8 hours long run was used to test for the effect of mechanical instabilities. For the analysis, the run was split into sections of about 1000 tracks. Fig. 7 shows the distributions of median residuals in x and y directions before the alignment updates.

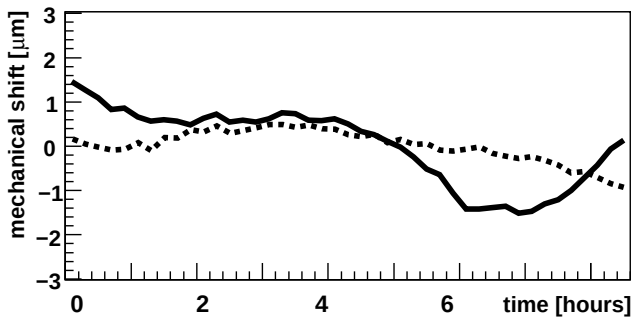

Figure 7: Mechanical shifts of Module 2 during an 8 hours' run. The plots show median residuals before re-alignment vs. time. Solid - vertical, dotted - horizontal direction.

Correction of positional response distortions The positional response distortion effects are in fact several different distortions that are treated by a common correction - "residual plot detrending": edge effects and other interstrip differences uncorrected by gain correction.

The correction improves tracking and leads to narrower distributions of residuals, which indicates that the correction is effective.

An example of such a plot before correction is in Fig. 8. The range of corrections is ± 20 μm for edge effects.

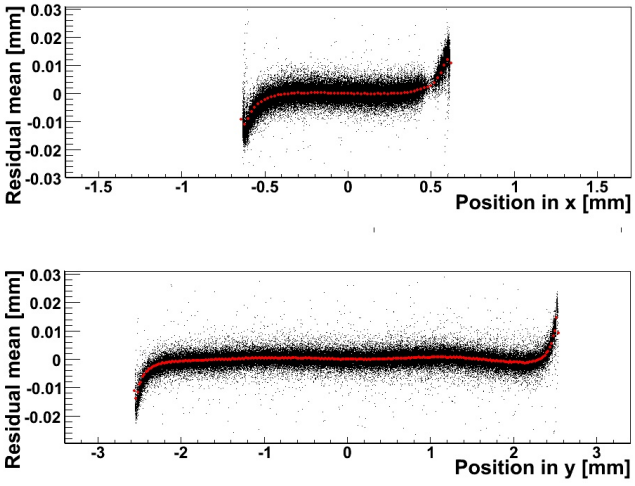

Figure 8: Residuals vs. hit position; positional response distortions before correction. Edge effect is clearly visible in both coordinates. The correction (light grey line) is based on median residuals at a given position.

Factors influencing resolutions: Summary Below we give our estimates of the impact of individual analysis steps on RMS residuals and resolutions of DEPFET detectors in the settings of the 2009 beam test (specifically, 120 GeV pion beam, and the given typical distance between detectors):

1. Gain correction (internal property of DEPFET): no observed influence
2. η - correction (single/double pixel η): influence on the level of 0.03 μm in y
3. Mechanical instability (running alignment on the timescale of tens of minutes): influence on the level of 1.0 μm.
4. Response distortions correction or edge cut 0.25 mm from detector perimeter (internal property of DEPFET): average influence in the range of 0.2 μm mostly on the perimeter
5. Removal of one module from analysis (setup and analysis property), influence on the level of 0.1 μm (assessed as a systematic error of analysis algorithm), repeatibility of analysis on similar data subsets is better than 0.01 μm.

7 Results and discussion II: Studies using resolutions

In this section, we present three typical beam test studies to illustrate the use of intrinsic resolutions.

7.1 Bias scan

For DEPFET sensors, the bias voltage is the voltage at the p^+ backside contact ("9" in Fig. 1). The bias scan was performed for voltages from 100 V to 200 V. The plot of resolutions versus bias voltage is shown in Fig. 9. The resolutions visibly stabilize above 160 V.

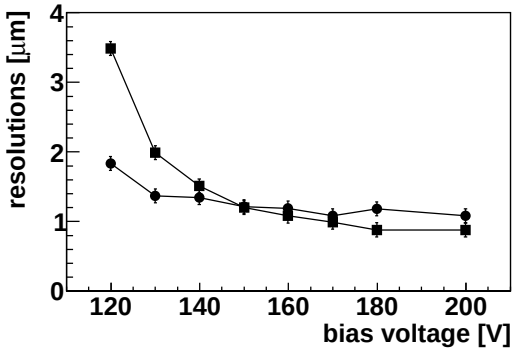

Figure 9: Bias scan: resolutions in x (circles) and y (squares) for the detector with pixel size 20 $\times$ 20 μm.

7.2 Angle scan

The angle scan was performed for a wide range of angles during the 2008 beam test. Here we only present the results for small tilts between -6° and 4° around y axis on the DUT (module 3). The results were already published in [15] and are reproduced here as a typical beam test study.

The results are summarized in Fig. 10. We conclude that tilt of a module affects all calculated values in a predictable

way. Residuals and resolutions are changed only in the x direction. While resolution gets worse at large tilts, small tilts increases charge sharing and cluster size, so that resolution improves.

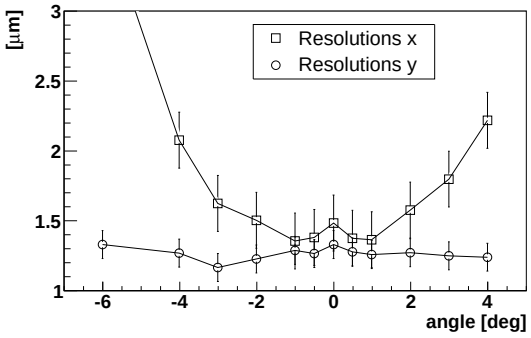

Figure 10: Resolution vs. incidence angle for the DUT with pixel size 24 × 24 μm in direction x (squares) and y (circles)

7.3 Energy scan

The energy scan was performed at the nominal beam energy of 120 GeV, with well-known particle and energy spectra, and at derivative energies of 100 and 80 GeV for pions, and 100, 80, 60 and 40 GeV for electrons. For all beam energies a good statistics for analysis has been acquired. However, the small acquisition rates at the lowest electron energies (61 and 33 minutes per 1000 tracks for 40 and 60 GeV electrons, respectively, versus 4.5 minutes for 120 GeV pions) mean that mechanical instabilities cannot be compensated as well as at higher energies. Moreover, the electron beam changed its position in space for different energies, which lead to mechanical transients from cabling and positioning stages. For these reasons, the results for electrons are not shown.

This scan is primarily a test of resolution estimates: the varying multiple scattering contribution must be properly unfolded from the measured residuals to give constant resolutions at all energies.

Figure 11 shows infinite energy extrapolation for pions superposed with actual resolutions calculated for the detector. Apparently, the extrapolation is in reasonably good agreement with the calculated resolutions.

8 Results and discussion III: Pixel mapping

Detector response was mapped against hit position within a (double) pixel. Such an analysis was performed for central detectors of the beam test setup with 20 × 20 μm pitch and 32 × 24 μm pitch.

Maps of resolutions within a sensor cell for the two detectors are shown in Fig. 12. Table 3 lists approximate ranges of variation of residuals and resolutions over the double-pixel area. Due to its fine pitch, detector 2 is better in both directions as regards homogenity of response.

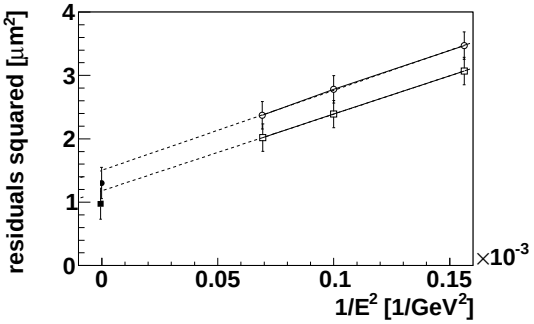

Figure 11: Squared residuals vs. squared inverse energy with extrapolation to infinite energy for pions: x, hollow circles; y, hollow squares. The solid marks at infinite energy are the respective intrinsic resolutions calculated directly.

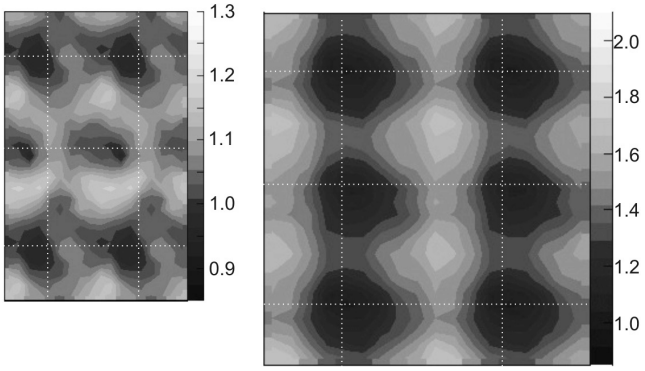

Figure 12: Maps of resolutions in pixel area (see also Table 3) for detector 2 (left, 20 × 20 μm pitch) and detector 3 (right, 32 × 24 μm pitch). Map dimensions correspond to pitch, but the grey scales are different.

We note that variation of resolution over the pixel area means that we have to update our definition of intrinsic resolution of a detector: it is the root-mean-square error of position measurement in a detector *averaged over pixel area*. The knowledge of pixel variations allows to improve hit reconstruction and tracking, which may be of interest in high-energy applications of the detectors.

9 Conclusions

This paper presents the results regarding intrinsic resolutions of the DEPFET pixel detectors based on the 2009 (and, in one experiment, 2008) DEPFET beam test(s) at CERN SPS.

We introduced the properties of the DEPFET detectors and explained how beam test data are analyzed.

We explained how intrinsic resolutions are calculated, and listed several factors influencing the resolutions. Of these, mechanical instabilities, which are unavoidable due to long measurement times, are important.

In particular, we have demonstrated that mechanical instabilities seriously complicate beam energy scans.

The influence of other factors affecting intrinsic resolutions

	Module	Approximate range, x	Appriximate range, y
Residuals	20 × 20 μm	1.4 - 1.6	1.2 - 1.5
in μm	32 × 24 μm	1.5 - 2.4	1.4 - 1.85
Resolutions	20 × 20 μm	1.0 - 1.2	0.8 - 1.2
in μm	32 × 24 μm	1.0 - 2.0	0.9 - 1.5

Table 3: Pixel-scale variation of residuals and resolutions.

can be excluded or limited by proper working settings for detectors and cautious analysis.

With our presentation of the bias scan, angle scan and energy scan, we intended to show that intrinsic resolution estimates behave regularly and are a reliable tool in detector studies.

Also, we show that intrinsic resolutions can be mapped on sub-pixel scales, and indeed vary on the scale of a pixel. Resolution mapping can help in providing more precise space points and errors by the detector for tracking in real high-energy physics experiments.

Acknowledgement

Zbynek Drasal, Zdenek Dolezal, Peter Kodys and Peter Kvasnicka were supported by the Czech Science Foundation Grant No. 203/10/0777, and by the Ministry of Education, Youth and Sports of the Czech Republic under contract No. LA10033 and MSM0021620859. Ariane Frey and Benjamin Schwenker gratefully acknowledge the support by the Volkswagen Foundation. Peter Fischer was funded by BMBF under Contract 05H09VH8.

References

[1] DEPFET homepage: www.depfet.org

[2] Kemmer, J., Lutz, G., *New detector concepts*, Nucl. Instrum. Meth. A, 253 (1987) 356

[3] Velthuis, J. J. et al., *DEPFET, a monolithic active pixel sensor for the ILC*, Nucl. Instrum. Meth. A, 579 (2007) 685-689

[4] Lutz, G. et al., *DEPFET-detectors: New developments*, Nucl. Instrum. Meth. A, 572 (2007) 311-315

[5] Fischer, P. et al., *Progress towards a large area, thin DEPFET detector module*, Nucl. Instrum. Meth. A, 582 (2007) 843-848

[6] Velthuis, J. J. et al., *A DEPFET based beam telescope with submicron precision capability.*, IEEE Trans. Nucl. Sci. 55 (2008) 662-666

[7] Kodys, P. et al., *Spatial resolution analysis of micron resolution silicon pixel detectors based on beam and laser tests.*, Nucl. Instrum. Meth. A 604 (2009) 385-389

[8] Kohrs, R.: *Development and characterization of a DEPFET prototype system for the ILC vertex detector.*, PhD. Thesis, Bonn University, 2008.

[9] Scott, G., Longuet-Higgins, H., *An algorithm for associating the features of two patterns*, Proc. Royal Society London, B244 (1991) 21-26

[10] Turchetta, R., *Spatial Resolution of Silicon Microstrip Detectors*, Nucl. Instrum. Meth. A, 335 (1993) 44-58

[11] ILC software/EUTelescope homepage: http://ilcsoft.desy.de/portal/software_packages/eutelescope/

[12] Furletova, J., Reuen, L.: *JRA1 - The DEPFET sensor as the first fully integrated DUT in the EUDET pixel telescope: The SPS test beam 2008*, EUDET-Memo-2008-34, December 2008, http://www.eudet.org

[13] Brun, R., Rademakers, F.: *ROOT - An Object Oriented Data Analysis Framework*, Nucl. Instrum. Meth. A, 389 (1997) 81-86. See also http://root.cern.ch/

[14] ILC software homepage: http://ilcsoft.desy.de

[15] Kvasnička, P., Nucl. Instrum. Meth. A, (2010). In press, doi:10.1016/j.nima.2010.06.170